Salt Effects on Solute Exchange and Micelle Fission in Sodium Dodecyl Sulfate Micelles below the Micelle-to-Rod Transition

Yahya Rharbi[†] and Mitchell A. Winnik*

Department of Chemistry, University of Toronto, 80 St. George Street, Toronto, Ontario, Canada M5S 3H6

Received: March 29, 2002; In Final Form: November 12, 2002

This paper describes micelle exchange kinetics of hydrophobic pyrene derivatives between SDS micelles in the presence of moderate concentrations of sodium counterions ([Na^+] < 150 mM). The kinetics were followed by fluorescence time-scan measurements in which the disappearance of excimer over time was monitored. The exchange rate constant k_{obs} is highly sensitive to the counterion concentration and increases as a power law against [Na^+] with an exponent of 4, from a value of almost 0 in the absence of salt to 10^{-2} s^{-1} for [Na^+] =100 mM. The exchange rate is not very sensitive to the concentration of SDS micelles, except as the SDS concentration affects the ionic strength, which indicates that the kinetics are dominated by a first-order process. This process is attributed to a fission−growth mechanism in which the fission rate is rate-limiting. Although fission can yield any size micelles, the use of hydrophobic probes restricts the observation to the events yielding two micelles large enough to bear the probe molecules. We propose that the barrier to fission is the creation of surface instabilities, which are enhanced in the proximity of the micelle-to-rod transition. Over the range of counterion concentrations investigated here, micelle fusion is inhibited by electrostatic repulsion.

Introduction

Sodium dodecyl sulfate (SDS) is one of the most important surfactants in common use. When one talks about surfactants and teaches undergraduates about micelle formation, SDS is almost always the first example that comes to mind. SDS self-assembles to form micelles when its concentration in water exceeds its critical micelle concentration (CMC) of 8.3 mM. Since it is an ionic surfactant, many of its micelle properties change when salts are added to its aqueous solutions. For example, the CMC decreases in the presence of salt, and the micelle size n_{agg} increases.[1−5] Values of n_{agg} at different salt and surfactant concentrations have been reported based on light scattering,[4] neutron scattering,[2] and fluorescence experiments.[3] Quina et al.[1] predicted a power law dependence of n_{agg} on the concentration of [Na^+] counterions at low ionic strength, with an exponent of 0.25. Bales et al.[6] provide an expanded discussion of this effect in the context of their electron spin resonance experiments on SDS micelles in the presence and absence of salt. Typically, n_{agg} for the micelles grows from ca. 60 to 90 when the counterion concentration increases from 20 to 140 mM. In this regime, the micelles remain spherical. For higher counterion concentrations, SDS undergoes a transition from having a spherical shape to being a wormlike micelle.[4−7] In the particular case of NaCl as the added salt, the transition to wormlike micelles was found by light scattering to occur at 0.5 M [Na+]. The polydispersity was reported to increase strongly in this regime.[7]

Like other micelles, the hydrophobic core of an SDS micelle is able to solubilize hydrophobic molecules in water. When the solute is a fluorescence dye, fluorescence experiments, can be used to characterize properties of the micelles, such as the mean aggregation number n_{agg}, as well as the polarity and the microviscosity in the region of the micelle where the dye resides.[8]

One of the most important characteristics of micellar systems is the dynamics of their formation and dissociation. Chemical relaxation techniques, such as stopped flow, pressure jump, temperature jump, and ultrasonic relaxation measurements have been used to examine many micellar systems.[9] In these techniques the system is rapidly perturbed to a nonequilibrium state by changing the temperature, pressure, or surfactant concentration. The relaxation to equilibrium is monitored by conductivity measurements if the system is ionic, or by light scattering, circular dichroism, or fluorescence measurements for nonionic micelles. These measurements frequently identify two well-separated relaxation times, a rapid relaxation that occurs on a time scale of microseconds and a slower process, which requires milliseconds to seconds. Most of our ideas about micelle dynamics were developed through the study of SDS micelles.[9−11] Aniansson and Wall[11] assigned the fast process to an association−dissociation process involving the exchange of individual surfactant molecules between the micelles and the water phase. This results in a change of the micellar size without affecting their number. They showed that one could calculate the exit k^- and reentry k^+ rate constants for the surfactant molecules from the concentration dependence of the fast relaxation time. They found that k^- was independent of the nature of the ionic group but strongly dependent on the hydrophobic group, and in most cases k^- deceases by a factor of more than 2 for every additional CH_2 group in the surfactant.[9c] The entry rate (with rate constant k^+) was found to depend very little on the structure of the surfactant. This is a diffusion-controlled process, and the magnitude of k^+ was found to range between 5×10^8 and 3×10^9 M^{-1} s^{-1}. In the particular case of SDS micelles, they reported $k^- = 10^7$ s^{-1} and $k^+ = 1.2 \times 10^9$ M^{-1} s^{-1}.[12] Aniansson and Wall[11] attributed the slow process to a sequence of steps involving the condensation or dissolution of individual surfactant

* To whom correspondence should be addressed. E-mail: mwinnik@chem.utoronto.ca.

[†] Current address: Laboratoire de Rheologie, CNRS (UMR 5520), Grenoble, BP 53 Domaine Universitaire, F 38041 Grenoble, France.

10.1021/jp020842f CCC: $25.00
Published on Web 01/28/2003

monomers, leading to the formation and breakdown of entire micelles. This process leads to a change of both the micellar size and the number of micelles present in solution. The rate-limiting step for the slow relaxation is the passage of the system through the minimum in the size distribution, separating surfactant monomers and the normal ("proper") micelles. This step is slow because the concentration of these intermediates is so low.

The model as developed by Aniansson and Wall did not take account of the counterion contribution, and thus pertained properly only to nonionic micelles. This model was extended to ionic micelles by Kahlweit and co-workers.[13] In this way, they were able to explain the decrease of the slow relaxation rate ($1/\tau_{slow}$) with increasing sodium ion concentration up to 60 mM [Na+]. At higher levels of salt, these authors found that a new process took over, with a rate that increased strongly with salt concentration. They proposed a mechanism in which submicellar species in the vicinity of the minimum of the size distribution coalesced to form proper micelles. By the law of mass action, this mechanism implies that proper micelles can spontaneously fission into submicellar aggregates. It has not been possible to observe either process directly. Experiments that measure relaxation kinetics provide clear evidence for a change in mechanism, but one must rely on models to try to distinguish different relaxation mechanisms.

We are interested in the use of fluorescent probes to study slow relaxation processes in surfactant micelles. Our basic hypothesis, which we describe in more detail below, is that the exchange of water-insoluble solutes among micelles involves micelle fusion or fission processes. As we have shown in a preliminary communication,[14] the use of a water-insoluble probe containing a pyrene chromophore allows one to study the fission kinetics of SDS micelles as influenced by the presence of the probe. These rates also increase strongly with increasing sodium ion concentration. One of our objectives is to understand the connection between solute exchange kinetics and micelle relaxation kinetics.

There is a broad interest in the topic of solute exchange between micelles.[15,16] Solutes with a significant water solubility exchange preferentially through an "evaporation−condensation" process, involving exit of the solute from the micelle into water, passage of individual solute molecules through the water phase, and capture by a different micelle. When the solute is a luminescent dye or a quencher, and the exchange occurs on the time scale of nanoseconds to hundreds of microseconds, the rate of this process can be studied by time-resolved fluorescence or phosphorescence quenching experiments.[17−23] These experiments have shown that the exit step is rate limiting, whereas the entry rates are close to diffusion controlled. Within a series of solutes containing a different number of aromatic rings or different alkyl substituents, the exit rate decreases rapidly with decreasing water solubility.[14,17]

In our approach,[24] we use as solutes the three pyrene-derivatives shown below: glycerol-1,2-distearate-3-pyrenebutyrate **1**, 1-dodecylpyrene (C_{12}Py), and 1-octylpyrene (C_8Py). We have used these probes to study solute-exchange kinetics for micelles of the nonionic surfactants Triton X-100 (TX100)[25] and Synperonic A7.[26] Solutions were prepared in which some micelles contain more than one molecule of probe. The fluorescence spectra of these solutions are characterized by a prominent excimer emission. When one of these solutions is mixed under stopped flow conditions with an excess of empty micelles, exchange takes place. One can follow this process in a time-scan experiment by monitoring either the growth in intensity of the blue "monomer" emission I_M or the decrease in intensity of the green "excimer" emission I_E.

CHART 1[a]

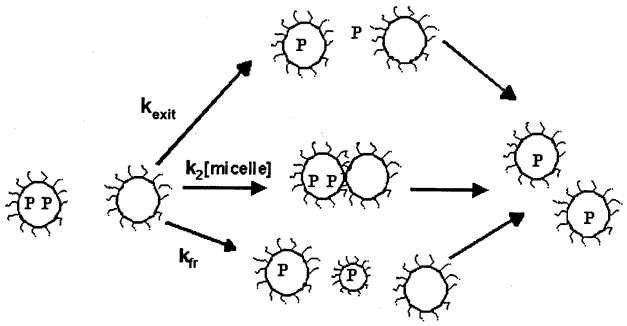

[a] (a) Exchange via water mechanism. (b) Collision−fusion−fission mechanism. (c) fission−growth mechanism.

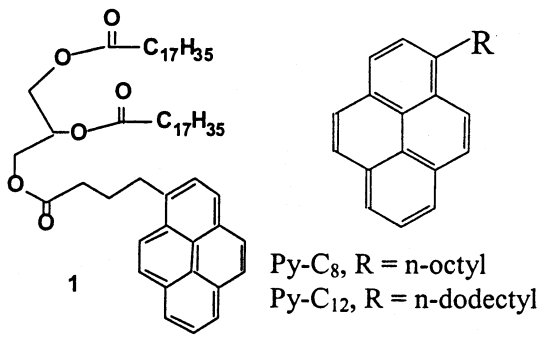

Chart 1 shows the three possible mechanisms for exchange of solutes that are solubilized by surfactant micelles. Here P refers to a generic solute and to a pyrene derivative that will give excimer fluorescence from micelles containing two P molecules. Exit−reentry (k_{exit}) is the dominant process for exchange of most solutes.[17] In our experiments, triglyceride **1** is so insoluble that this path is suppressed. The middle path (collision−fusion−fission, k_2) will exhibit kinetics second order in micelle concentration, and the lower path (fission−growth, k_{fr}) will exhibit first-order kinetics.

When the solute has a very low solubility in water, the exit-re-entry mechanism for solute exchange will be suppressed ($k_{exit} \approx 0$). Hilczer et al.[27] recently developed a detailed theoretical model to describe the kinetics of solute exchange by the mechanisms shown in Chart 1. In their model they treat explicitly the changes in monomer and excimer fluorescence intensity that accompany the exchange of pyrene-type solutes, including the case in which some micelles contain more than two solutes. In this case, more than one exchange step is necessary for disappearance of the excimer emission.

In TX100, the dominant process of solute exchange involves micelle fusion.[28] This process occurs with a second-order rate constant $k_2 = 2.9 \times 10^6$ M^{-1} s^{-1} at 24.6 °C and an activation energy of 160 kJ/mol. The other mechanism was found to be independent of the concentration of empty micelles. It was attributed to the fission−growth process, in which a micelle spontaneously divides into two smaller entities ("submicelles"). These smaller aggregates then grow into normal micelles by fusion with other submicelles or by condensation of surfactant monomers. For **1** in TX100, $k_{fr} = 10$ s^{-1} at 24.6 °C with an activation energy of 110 kJ/mol.

In this paper, we extend these measurements to the study of solute exchange in SDS micelles. Our experiments recall a similar experiment reported more than a decade ago by Bohne

and Scaiano,[29] who observed a very slow exchange of C_{12}Py between SDS micelles in water. We examine the influence of salt and surfactant concentration on the solute exchange rate, focusing, on the low salt regime, with [NaCl] ranging from 0 to 0.14 M, and [SDS] from 15 mM to 75 mM. In the range of salt concentrations we examined, the exchange of **1** was dominated by the fission−growth mechanism. In contrast, C_8Py and C_{12}Py, despite their low intrinsic solubility in water, appear to exchange by the exit−reentry mechanism.

This paper is organized as follows: After the Experimental Section, we first describe the preparation and characterization of solutions of **1** in SDS micelles. We then describe the changes that occur when salt is added rapidly to these solutions and interpret the results in terms of the mechanism of solute exchange. We compare our results to the classic results by Kahlweit and co-workers[13] on the effect of salt on the slow relaxation kinetics of SDS micelles. Finally, we consider the role of shape fluctuations to explain the effect of salt on the spontaneous fission of SDS micelles.

Experimental Section

Materials. The molecule **1** (M_w = 882) is a triglyceride in which 4-(1-pyrene)-butyric acid is one of the constituent fatty acid esters. Its synthesis and characterization is described elsewhere,[32] as are the syntheses and characterization of 1-octyl pyrene and 1-dodecyl pyrene sodium dodecyl sulfate (SDS, Aldrich) and sodium chloride (NaCl, Aldrich) were used as received. Distilled water was further purified through a Millipore Milli-Q purification system.

Surfactant Solutions Containing Pyrene Derivatives. To prepare solutions of **1**, octyl pyrene and dodecyl pyrene in aqueous solutions of SDS micelles, we used an indirect method. Aqueous solutions of Triton X-100 (21.66 g/L) were mixed with 0.1 mg of each of the pyrene derivatives. Each mixture was heated at 75 °C (above the cloud point) and strongly agitated for 15 min with a Vortex Genie 2 model G 560 mechanical shaker at its maximum frequency (>10 Hz). The solution was allowed to cool to room temperature over 2 h and then filtered through a 0.2 μm filter in order to remove undissolved probe. These transparent solutions were each diluted with aqueous TX100 surfactant solution and with water to yield stock solutions containing 0.68 mM of TX100 and ca. 2.15 μM Py-R. To 10 mL of each solution, a concentrated SDS solution (11, 24, 36, and 46 g/L) was added and the mixture was stirred at room temperature for 1 h. Each final solution contains [Py-R] $\approx$ 1.075 μM in a mixture of TX100/SDS = 1/250 and with initial SDS concentrations of 21, 43, 65.7, and 86 mM. The fluorescence emission of each mixture remained stable for a few days. The amount of Py-R solubilized in each TX100 solution was determined by UV absorption measurements (Hewlett-Packard 8452A diode-array spectrometer. 1.00 cm cell) at 346 nm, using $\epsilon_{346} = 3.0 \times 10^4$ M^{-1} cm^{-1} determined previously. The background was subtracted using a TX100 solution of the same concentration as a reference. The absorbance of each of Py-R at 346 nm was calculated relative to that at 398 nm, which was considered as the base line.

Fluorescence Measurements. Static fluorescence measurements were carried out with a SPEX (2.1.2) Fluorolog spectrometer in the S/R mode. The signal intensity was kept below 2×10^6 counts/s to maintain the linearity of the detector response. For emission spectra and for time-scan kinetics experiments, λ_{ex} = 346 nm, whereas excitation spectra were obtained for both λ_{em} = 375 nm (monomer) and λ_{em} = 480 nm excimer). Fluorescence decay profiles of excited pyrene were measured by the single-photon-timing technique with λ_{ex} = 346 nm and λ_{em} = 375 nm. The excitation source was a coaxial flash lamp (Edinburgh instrument model 199 F) filled with deuterium.

Micelle Characterization. Fluorescence decay profiles were fitted to the Tachiya-Infelta Poisson quenching model.[30] The fitting parameters in this analysis are the intensity at time zero I_o, the average number of molecules of Py-R per micelle $\langle n \rangle$, and the pseudo-first-order rate constant for excimer formation k_Q.

$$I(t) = I_0 \exp[t/\tau_0 - \langle n \rangle (1 - \exp(-k_Q t))] \quad (1)$$

The unquenched lifetime τ_0 is known independently from experiments at low [**1**] by fitting these decay to an exponential expression. When the data were fitted to eq 1 with four fitting parameters, the value of the unquenched pyrene lifetime τ_o was essentially identical to that measured at low probe concentration. The aggregation number n_{agg} is calculated from the slope of the plot of $\langle n \rangle$ vs Py-R concentration

$$\langle n \rangle = [\text{pyrene}] n_{agg}/([\text{surfactant}] - \text{cmc}) \quad (2)$$

Kinetics Experiments. In measurements of the exchange kinetics, two solutions were mixed in the sample chamber of a home-built stopped-flow injector with dead time 2 ms. Details about the instrument are provided in ref 28. In each injection, 0.35 mL of a solution containing [Py-R] in the range of 2.5 μM + SDS (0.68 mM) was mixed with 0.35 mL of a solution with [NaCl] varying from 0 to 300 mM. Experiments were carried out at room temperature, 23 °C. The signal was monitored at either λ_{em} = 375 nm or λ_{em} = 480 nm, with integration and interval times of 1 ms to 10 s and a total experiment time ranging from 1 to 10000 s. In other experiments, solutions of **1** in [TX100] were mixed with [SDS] solutions in a similar fashion. Decay profiles were fitted to an exponential function or to a sum of two exponential terms.

Results and Discussion

Formation and Characterization of Py-SDS Solutions. It is very difficult to prepare solutions in SDS micelles of molecules with a low intrinsic water solubility. To overcome this problem, we used an indirect approach based on Dubin's studies[31] of SDS mixed micelles to prepare solutions of pyrene derivatives (Py-R) in aqueous SDS micelles. The Py-R derivatives were first dissolved in TX100 micelles under conditions in which the probe achieved a Poisson distribution among these micelles.[32] These solutions, with a mean occupancy $\langle n \rangle$ ranging from 0.5 to 2.5, were then mixed with a large excess of SDS in water. Individual surfactant molecules exchange rapidly between the different kinds of micelles. In many of our experiments the solution of the probe in TX100 (0.68 mM) is mixed with an equal volume of SDS solution (160 mM). For such a low TX100 to SDS ratio (1:230), one expects the TX100 to be randomly partitioned between water and SDS micelles.[31] If the SDS micelles have an aggregation number of 50, one micelle in 5 will contain one molecule of TX100. In this section, we provide evidence to support the idea that the pyrene derivatives are located in an SDS environment.

In Figure 1, we show a fluorescence spectrum of a solution of **1** in water in the presence of 0.68 mM TX100 prior to and after addition of SDS solution (160 mM). Both spectra are characterized by a broad excimer emission with a peak at 480 nm, in addition to the monomer fluorescence with a (0,0) band at 375 nm. These freshly prepared solutions were examined by

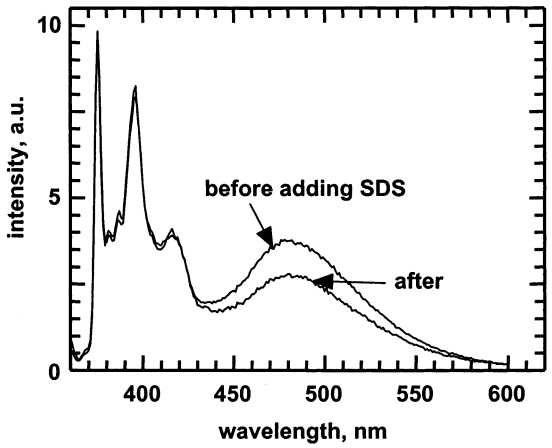

Figure 1. Emission spectra ($\lambda_{ex} = 346$ nm) of **1** solubilized in aqueous solutions of micelles. In the spectrum labeled "before adding SDS," [**1**] = 2.15 μM and [TX100] = 0.68 mM. The spectrum "After" refers to the solution obtained by mixing the original solution with an equal volume of SDS (160 mM).

fluorescence decay measurements. Solutions containing various concentrations of **1** in TX100 (0.68 mM) in atmospheric air were examined by fluorescence decay measurements. The pyrene fluorescence decays fit the Poisson quenching model (equation 1) with a lifetime $\tau_o = 170$ ns similar to that recovered from fitting fluorescence decay profiles of dilute solutions of **1** to a single exponential. The first-order rate constant for excimer formation k_Q is almost constant for all ratios **1**/[TX100] and equal to 3.5 μs^{-1}. When aliquots of a concentrated SDS solution (160 mM) were mixed with this solution, the measured fluorescence decay profiles could not be fitted to eq 1 with an unquenched lifetime of 170 ns, but instead fit with $\tau_o = 130$ ns. When NaCl was added to this solution, the excimer disappeared and the decay fit to an exponential expression with a similar lifetime, $\tau = 130$ ns. To obtain further information, both experiments were repeated in solutions deaerated with nitrogen. Under these circumstances, the decay profiles fit to eq 1 with unquenched lifetimes of 228 ns, both before and after addition of SDS. Thus the change in this lifetime is due to quenching by oxygen, and the rate of this quenching is more rapid in the system containing SDS.

The first-order rate constant for excimer formation k_Q, is related to the microfluidity of the pyrene environment. TX100 micelles have a more rigid core than that of SDS,[33] and previous experiments have shown that the rates of excimer formation from pyrene and from 1-ethylpyrene were 5−10 times higher in SDS (30 μs^{-1}) than in TX100 (3.5 μs^{-1}). Here we found k_Q, after addition of SDS, to be 3 times larger for **1** than its value in pure in TX100 (3.5 μs^{-1}) (Figure 2). These results confirm that the environment of **1** has changed after addition of SDS, from sites characterized by low microfluidity (TX100) to new sites of higher microfluidity. Therefore we conclude that the environment of **1** is the core of SDS micelles.

The TX100/SDS exchange process is itself rather subtle. The system initially contains TX100 micelles with a mean aggregation number of about 100, and after SDS addition forms SDS micelles with a mean aggregation number of about 50. The recovered $\langle n \rangle$ values from the fluorescence decay measurements after addition of SDS become half of those obtained in pure TX100 (Figure 2B). Stopped-flow kinetic measurements show that this rearrangement of the system occurs on a very rapid time scale at the very limit of our ability to detect it. Upon rapid mixing of solution of **1** in TX100 (0.68 mM) to a SDS

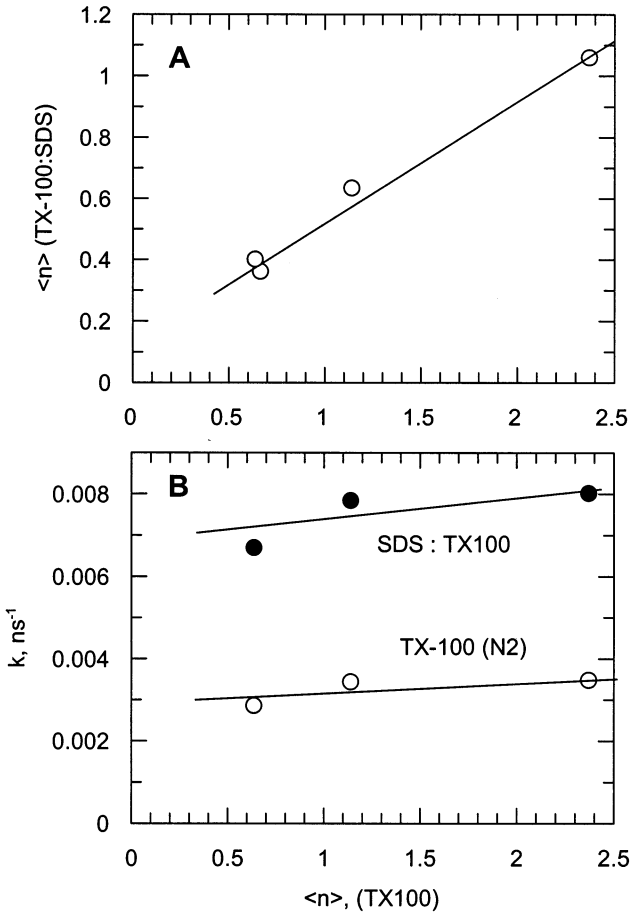

Figure 2. The fitting parameters k_q and $\langle n \rangle$ from the analysis of measured fluorescence decay profiles for **1** in TX100 micelles (0.68 mM) before and after addition of an equal volume of SDS (160 mM). In (a), the mean occupancy number $\langle n \rangle$ found for the solutions after addition of SDS is plotted against the $\langle n \rangle$ values determined prior to addition of SDS. In (b), the corresponding values of k_Q [(O) no SDS; (●) after SDS addition are plotted vs the $\langle n \rangle$ values determined prior to addition of SDS.

solution 160 mM, the excimer I_E (480 nm) and monomer I_M (375 nm) intensities change at a fast rate, and then remain unchanged for a period of days. When we mix this TX100 solution with more concentrated SDS solutions, following the rapid response, I_E decreases and I_M increases over a period of hours to minutes depending on [SDS]. At the end of this process, the fluorescence spectrum shows no discernible excimer and a strong monomer band compatible with the absence of pyrene in the excimer state (Figure 3). This result is consistent with repartition of the pyrene among the SDS micelles in such a way that the probability of two molecules of **1** occupying the same micelle is insignificant.

In Figure 4 we show the exchange experiment in which we monitor the intensity of the excimer peak I_E upon stopped-flow mixing of the of aqueous solutions of **1** in TX100 with various concentrations of SDS. When these decays were fitted to a single-exponential expression, we recovered decay times varying from hours at low [SDS] to minutes at higher [SDS]. When the kinetics was monitored at the monomer peak I_M, similar decay lifetimes were recovered. This process is much slower than the exchange rate of the individual surfactant molecules. From ultrasonic experiments, the exit rate constant of the single surfactant molecule was reported to be $k^- = 0.11 \times 10^7$ s^{-1} for TX100 and $k^- = 1 \times 10^7$ s^{-1} for SDS.[11,34] The entry rates are diffusion controlled with a rate constant $k^+ = 3.7 \times 10^9$

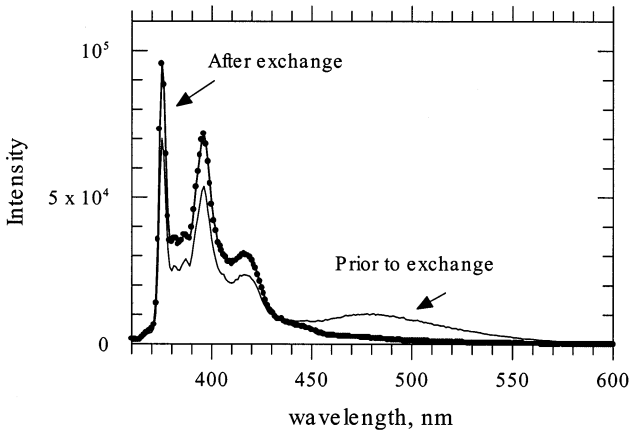

Figure 3. Emission spectra (λ_{ex} = 346 nm) of **1** solubilized in aqueous solutions of SDS micelles. The spectrum labeled "Prior to exchange" ([**1**] = 1.1 μM and [SDS] = 140 mM) refers to the sample measured few minutes after mixing a solution of **1** in TX100 with a solution of SDS. The spectrum "After exchange" refers to the spectra measured after 2 days.

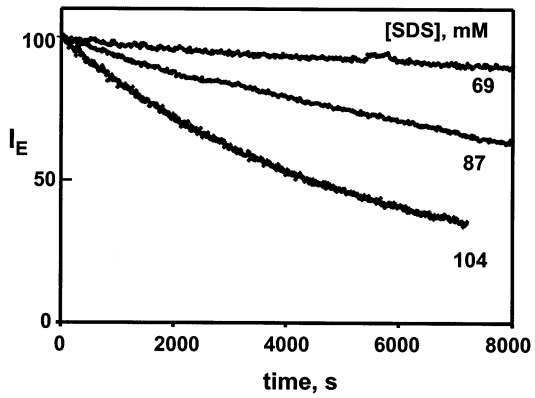

Figure 4. Time-scan experiments monitoring the decrease in the excimer emission I_E (λ_{em} = 480 nm) after mixing a solution of **1** in TX100 micelles ([**1**] = 1.1 μM; [TX100] = 0.68 mM) with an equal volume of SDS solution ([SDS]] = 138, 174, and 208 mM) at 23 °C.

M^{-1} s^{-1} for TX100 and 1.2 × 10^9 M^{-1} s^{-1} for SDS.[35] Following the mixing of the two solutions, surfactant molecules exchange rapidly via the exit-condensation mechanism, while the exchange of the Py-R solutes occurs on a much longer time scale. When we repeated the exchange experiment using less hydrophobic pyrene derivatives, the exchange process was found to be much faster than that of **1**: minutes for C_{12}Py, and seconds for C_8Py.

Solute Exchange in SDS Micelles. Chart 1 illustrates three different mechanisms for exchange of solutes between micelles. In any given exchange experiment, all three mechanisms could occur simultaneously. Since the rates of these processes have different sensitivities to surfactant and salt concentration, their individual contribution can be separated. For example, the exchange-via-water and the fission−growth mechanisms are characterized by first-order kinetics, whereas the collision-fusion−fission mechanism should exhibit second-order kinetics with a second-order rate constant k_2 and a pseudo-first-order exchange rate constant k_{obs} dependent on the concentration of empty micelles.

For the solute exchange experiment, the SDS solutions were prepared from TX100 solutions with a low mean occupancy of probes per micelle. We interpret the data in Figure 3 to indicate that the method of sample preparation creates SDS micelles in which a small fraction contains two probes and a negligible fraction contains three or more probes. When this solution is mixed with an excess of empty micelles, the fraction of micelles $P(t)$ bearing a pair of Py-R should decrease exponentially with time, with a rate characterized by a pseudo-first-order rate constant k_{obs}, which contains contributions from all three exchange processes.

$$I_E \propto P(t) = P(0)\exp(-k_{obs}t) \quad (3)$$

$$k_{obs} = k_{exit} + k_{fr} + k_2[\text{micelle}] = k_{exit} + k_{fr} + k_2([\text{SDS}] - \text{cmc})/n_{agg} \quad (4)$$

Here k_{exit} describes the exit rate constant of the solute from the micelles; k_{fr} describes the fission rate constant monitored through the decay of I_E; and k_2 describes the collision−fusion−fission rate. For a given micelle containing two probes, a single event of fission or fusion−fission could have two outcomes. Both probes may remain in one micelle, leaving the other one empty; or each probe could occupy one of the micelles. Only the second process can be observed in our experiment. In the fusion−fission process, the true rate constant for this process is twice the experimental value of k_2. The situation for fission is more subtle, since only a fraction of the fragments are large enough to solubilize a probe.

Effect of Salt Concentration. We have reported previously that the exchange of the Py-R molecules in TX100 micelles occurs mainly through a fusion−fission mechanism.[25] This process is favored by the low energy barrier to fusion due to steric repulsion between the micelles. In ionic surfactant micelles, the barrier to close contact is caused by electrostatic repulsion due to charges on the micelle surface. According to DLVO theory,[36] an increase in the ionic strength leads to screening of the electrostatic charge, which should lower the energy barrier to close contact. Following this idea, we examined the effect of salt on the exchange process.

To proceed with these experiments, we begin with a solution of **1** in aqueous SDS ([**1**] = 1.1 μM; [SDS] = 80 mM) prepared as described above. Aliquots of this solution, which exhibited both excimer and monomer emission, were mixed with equal volumes of aqueous solutions of NaCl. In Figure 5A, we show the results of two time-scan experiments in which we monitor the decrease in excimer emission intensity (I_E, 480 nm) and the increase in monomer emission intensity (I_M, 375 nm) following rapid mixing. The system responds on two separate time scales. On the time scale of one or two seconds, we observe an increase in I_E and a decrease in I_M. This response is followed by a pronounced but slow decrease in I_E, accompanied by an increase in I_M, until the excimer emission disappears (Figure 5B). The long-time behavior is due to the migration of **1** from the full to empty micelles. The short-time behavior reflects a more complex response of the influence of salt on the structure of the SDS micelles.

When these curves are fitted to a difference in two exponential terms, the fast rising component is obtained with relatively poor precision, whereas the slow decay is obtained with excellent precision. Both the monomer and excimer curves give similar decay rates. Since the two events happen on such different time scales, the relaxation rate of the long decay can be obtained equally well by fitting the data after 20 s to a single-exponential function. The thin solid lines drawn through the long excimer decays in Figure 5A,B represent an exponential fit to the data. Since the excimer decay gives data with higher precision (the weighted residuals from these fits are less than 5%), we use these data to calculate values of the exchange rate constant k_{obs}.

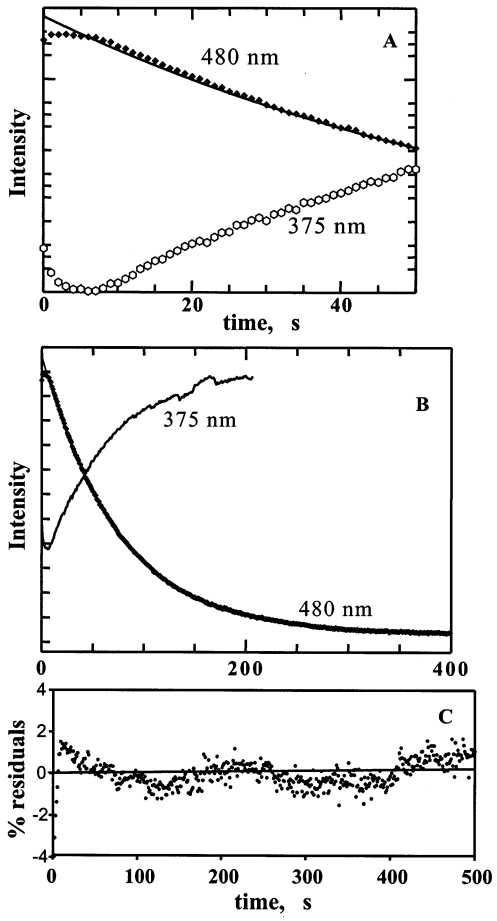

Figure 5. Time-scan experiments monitoring the increase in the monomer emission I_M ($\lambda_{em} = 375$ nm) and the decrease in the excimer emission I_E ($\lambda_{em} = 480$ nm) after mixing a solution of **1** in SDS micelles ([**1**] = 1.1 μM, [SDS] = 80 mM) with an equal volume of NaCl solution ([NaCl]] = 0.2 M) at 23 °C. The solid lines represent the exponential curves that best fit the data. (A) Expanded time scale emphasizing the response at short times. (B) The full data set measured over 400 s. (C) Weighted residuals from the best fit of the excimer data to an exponential curve.

When the exchange experiments are repeated with different salt concentrations, we notice a strong dependence of the exchange rate on the concentration of NaCl (Figure 6). The rates of the short-time and long-time processes both increase with increasing salt concentration.

Short-Time Process. We attribute the short-time process to a change in the micelle structure caused by dilution and the increase in the salt concentration. The salt concentration influences the micelle structure and the properties of pyrene probes in the micelle in several ways. Increased salt concentration leads to an increase in the micelle size. It can affect the location of the pyrene probe in the micelle, and it can affect the microfluidity of the micelle environment. The increase in I_E and decrease in I_M seen at short times are most likely due to an increase in the rate constant for excimer formation k_Q of **1**.

Lianos et al.[37] used pyrene as a probe and monitored the effect of [Na^+] on the emission peak intensity ratio I_1/I_3, a measure of the polarity of the probe environment. They inferred that increased salt concentration leads to a decrease in the core polarity of SDS micelles. This change may also be accompanied by an increase in the core microfluidity, resulting in an increase in k_Q. On the other hand increasing the salt increases the micelle aggregation number from 57 at 25 mM NaCl to 87 at 140 mM NaCl.[1−8] This growth in micelle size reduces the pyrene-pyrene

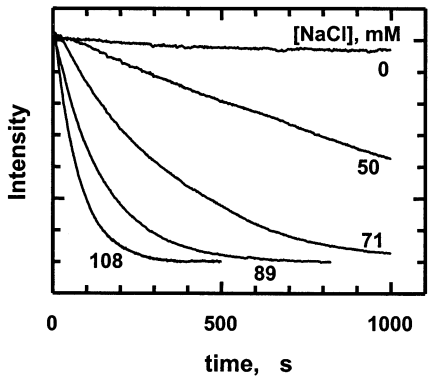

Figure 6. Time-scan experiments at 23 °C monitoring the decrease in I_E after mixing a solution of **1** in SDS micelles ([**1**] = 1.1 μM, [SDS] = 80 mM) with an equal volume of NaCl solutions at various concentrations ranging from 0 to 0.2 M. The final NaCl concentration for each solution is indicated on the plot.

encounter probability, which reduces k_Q. The small increase in k_Q that we infer at short times in the stopped-flow mixing experiments upon addition of salt could result from the competition between an increase in the core microfluidity and a decrease in the encounter probability.

In every case we examined, the fast process terminated within 1/10 of the time of the decay associated with exchange. The rapid process led to a change in excimer intensity less than 15% of that produced by solute exchange. We are confident of our ability to separate the kinetic contributions of both processes.

Long-Time Process. The slow relaxation is the result of migration of **1** between micelles. Both the monomer and the excimer decays fit to an exponential expression with the same rate constant. In Figure 7A, we show the influence of the surfactant concentration on the exchange rate constant. The relaxation rates k_{obs} calculated from the fit of the individual I_E decays remains very small until the SDS concentration reaches 50 mM, and increases for [SDS] > 80 mM: k_{obs} increases from almost 0 at low [SDS] to 1.8×10^{-3} s^{-1} for [SDS] = 104 mM. In Figure 7B, we show the influence of salt concentration on the exchange rate constant. For experiments carried out at 40 mM SDS, k_{obs} varies between essentially zero for no added salt to 0.045 s^{-1} for [NaCl] = 0.14 M (Figure 7B).

It is well-appreciated that the size and the structure of SDS micelles depends primarily on the counterion concentration. Quina et al.[1] and Almgren et al.[3] have shown that the aggregation number n_{agg} of SDS micelles varies as power law with the free counterion concentration, with an exponent $\gamma = 0.25$.

$$n_{agg} = n_o([Na^+]_{aq})^{\gamma} \quad (5)$$

Here n_o is the aggregation number of SDS at the cmc in the absence of added salt. From their analysis of data in the literature, Bales et al.[6] inferred that $n_o = 50 \pm 4$. The value of [Na^+]$_{aq}$, the free sodium ion concentration in the aqueous phase, is given by[5]

$$[Na^+]_{aq} = \alpha([SDS] - [SDS]_{free}) + [SDS]_{free} + [NaCl] = \alpha[SDS] + \beta[SDS]_{free} + [NaCl] \quad (6)$$

where [SDS]$_{free}$ is the unbound surfactant monomer concentration in the solution, α is the degree of dissociation of the SDS micelles, and $\beta = 1 - \alpha$. [SDS] is the total surfactant concentration. The value of α was estimated from activity measurements[38] to be 0.27. The cmc of SDS decreases upon

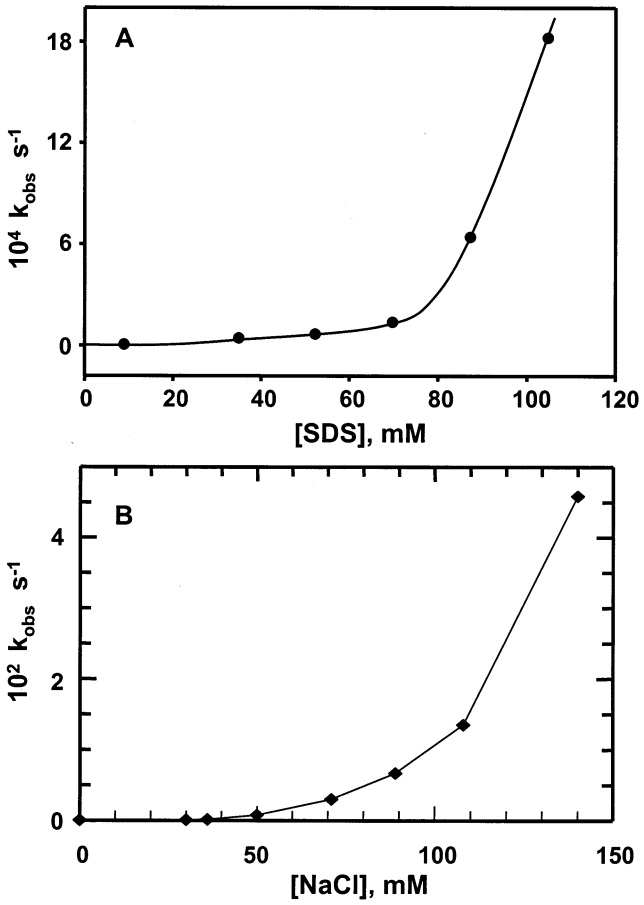

Figure 7. (A) The relaxation rate constants k_{obs} for **1** calculated from the fits of the data from individual stopped-flow experiments plotted vs the concentration of SDS. The experiments were carried out in the absence of added NaCl. (B) The relaxation rate constants k_{obs} for **1** plotted against the concentration of NaCl. These decays were monitored at $\lambda_{em} = 480$ nm with $\lambda_{ex} = 346$ nm. In these experiments [SDS] = 80 mM.

addition of salt, following the expression[39]

$$\log(\text{cmc}) = -A_1 - A_2\log(\text{cmc}_o + [\text{Na}^+]_{\text{added}}) \qquad (7)$$

where $[\text{Na}^+]_{\text{added}}$ is the molar concentration of added salt, $A_1 = 3.6$, and $A_2 = 0.678$. Equation 5 was found to describe the dependence of n_{agg} on both salt and surfactant concentrations. In Figure 8, we present a log−log plot of the dependence of k_{obs} on the total sodium ion concentration in the solution. Our data exhibit a power-law dependence with an exponent of 4. The power-law exponent obtained from our experiments indicate a much stronger dependence on $[\text{Na}^+]$ than that associated with the increase in micelle aggregation number.

Identifying the Exchange Mechanisms. At first glance, one might be tempted to attribute the increase in the exchange rate constant with increasing salt concentration to a second-order exchange process. One might imagine that the rate of this process would increase because of the reduction in the electrostatic repulsion between micelles. To examine this idea, we carried out experiments in which we varied the concentration of added empty SDS micelles, while keeping the salt concentration fixed at [NaCl] = 0.14 M. In Figure 9, we plot values of k_{obs} vs the total concentration of micelles. The micelle concentration was determined from the surfactant concentration and the value $n_{agg} = 87$[1−8] at this salt concentration. This plot shows a rather weak dependence of the exchange rate constant on (empty) micelle concentration, and a very important first-order

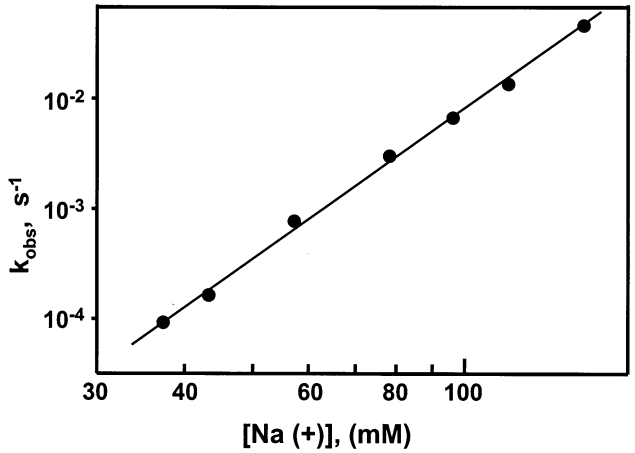

Figure 8. The data from Figure 7 replotted in log−log form against the free counterion concentration $[\text{Na}^+]_{aq}$. Values of $[\text{Na}^+]_{aq}$ were calculated from [NaCl] using eq 6.

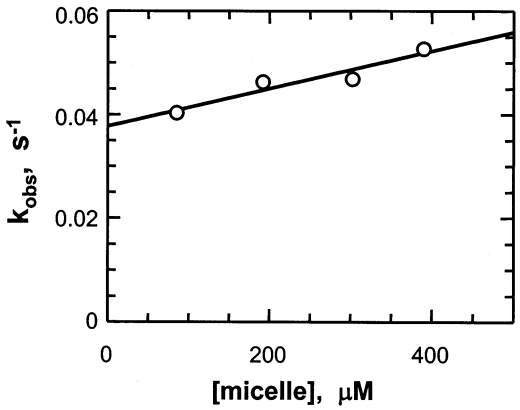

Figure 9. The relaxation rate constants k_{obs} for **1** calculated from the fits of the data from individual stopped-flow experiments plotted vs the concentration of SDS micelles. In this set of experiments the concentration of NaCl is 0.14 M.

contribution to the exchange rate. This situation is very different than that found for TX100, where the exchange of **1** was dominated by the fusion−fission process.[25]

Second Order vs First-Order Kinetics. The plot in Figure 9 is characterized by a slope of 38 M^{-1} s^{-1} and an intercept of 0.037 s^{-1}. These experiments were not carried out at constant $[\text{Na}^+]$. Although each solution, after mixing in the stopped flow apparatus, contained 140 mM NaCl, the different samples had different amounts of SDS. As a consequence, there are two ways to explain the dependence of the rate on the concentration of SDS micelles. On one hand, one can treat k_{obs} as a pseudo-first-order rate constant. Under these circumstances, the slope indicates a small second order contribution to the exchange rate. On the other hand, the increase in SDS micelle concentration makes a small but possibly significant contribution to the total sodium ion concentration. This increase could lead to an increase in k_{obs}, which would still describe a first-order exchange process. In our earlier communication,[14] we favored the latter explanation. We felt that if the exchange process followed a mechanism, which depended upon the sodium ion concentration as described by eq 6, we should observe a power law dependence of the exchange rate constant on $[\text{Na}^+]$. In Figure 10 we replot the data (k_{obs} vs $[\text{Na}^+]$) from Figure 7A,B in log−log form, and show that both sets of data define a common line, for values of k_{obs} varying over more than 5 orders of magnitude. From this perspective, it appears that the dependence of the exchange rate constant on [SDS] is due only to the enhancement of the first-

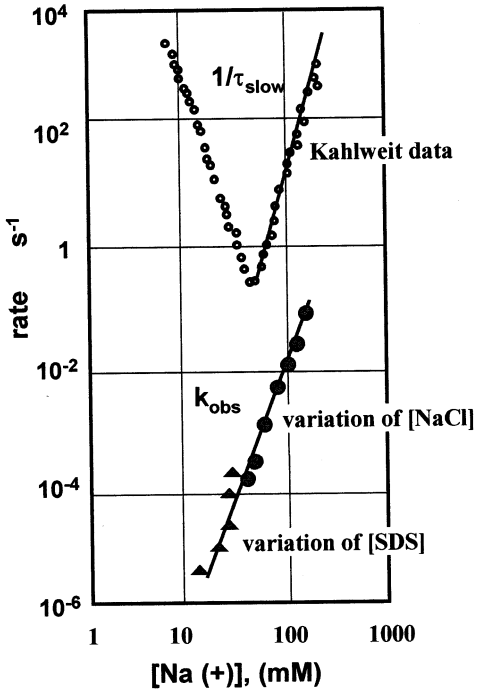

Figure 10. The data from Figure 7A,B are combined and replotted in log−log form against the total counterion concentration. These values are compared to the slow rate from the chemical relaxation experiments reported by Lessner et al. in ref 13b.

order process by increasing the concentration of counterions in the solution, and the electrostatic repulsion is still sufficient to inhibit close contact between micelles.

In more recent experiments to be published separately,[40] we find that there is a significant second-order contribution to the exchange rate at higher salt concentrations. Thus the small slope seen in Figure 9 may be a weak vestige of this second-order rate.

Exit−Reentry vs Fission−Growth. In this section, we try to distinguish between two distinct first-order exchange mechanisms: exit−reentry, in which the probe passes through the water phase to enter a different micelle, and fission−growth, in which the micelle splits into two smaller submicelle species, which then grow to normal size. Since the reentry rate constant is diffusion controlled (with $k^+ \approx 3 \times 10^9$ M^{-1} s^{-1} in water), the rate of exchange of dyes through exit−reentry is determined by the solute exit rate constant from the micelles. The exit rate constant can be calculated from the equilibrium solubility using the expression

$$k^- = k^+[P]_w/n^* \quad (8)$$

where $[P]_w$ is the water solubility of the solute, and n^* is the average number of solutes per micelle at the solubility equilibrium.

This exit rate constant should decrease as the salt concentration increases. First, one expects n^* to increase. For a series of experiments at constant probe and surfactant concentrations, the increase in n_{agg} leads naturally to an increase in the mean micelle occupancy. Second, increasing the ionic strength should lower $[P]_w$ (a salting-out effect). Our results show that the exchange rate constant k_{obs} for **1** increases strongly with an increase in $[Na^+]$ (Figure 10). We conclude that the exchange of **1** between SDS micelles does not occur by exit of **1** into the water phase.

When we repeated these experiments with the pyrene derivatives C_8Py and C_{12}Py**,** we find very different results. For

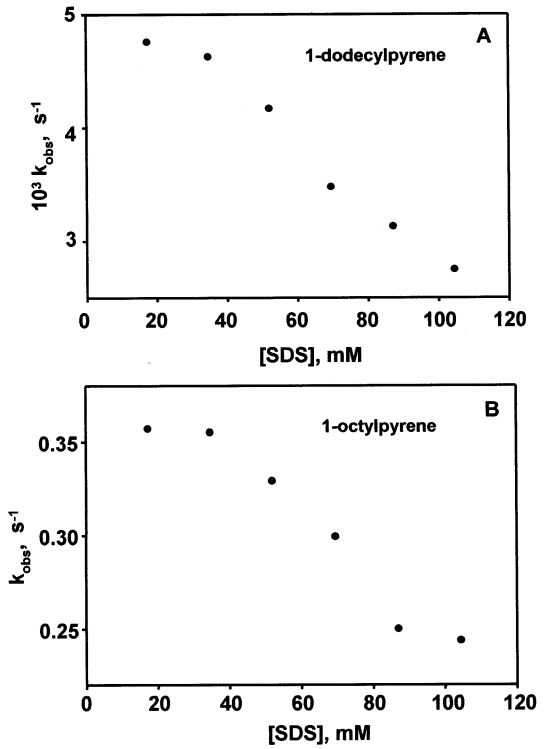

Figure 11. The relaxation rate constants k_{obs} of Py-R calculated from the fits of the data from the individual stopped-flow experiments plotted against the concentration of SDS. The experiments were carried out in the absence of added NaCl. The decays were monitored at $\lambda_{em} = 480$ nm with $\lambda_{ex} = 346$ nm. (A) 1-octylpyrene and (B) 1-dodecylpyrene.

both probes, k_{obs} was found to decrease with increasing sodium ion concentration. In Figure 11 we show the results for the exchange rate of C_{12}Py and C_8Py as a function of [SDS]. For C_{12}Py, k_{obs} decreased from 5×10^{-3} s^{-1} to 2×10^{-3} s^{-1} when [SDS] increased from 20 to 100 mM. Under the same conditions, k_{obs} for C_8Py decreased from 4×10^{-1} to 2×10^{-1} s^{-1}. We infer that the exchange of these probes, under these conditions, is dominated by the exit-reentry mechanism.

The conclusion that the exchange of C_{12}Py proceeds by unassisted passage through the water phase differs from the interpretation originally put forward by Bohne and Scaiano.[29] Thus a few more comments about this conclusion are warranted. It is very difficult to measure $[P]_w$ directly for molecules with low equilibrium water solubilities. An alternative is to try to estimate water solubility based on simple group-additivity rules. For example, the presence of two additional CH_2 groups decreases the water solubility of simple hydrocarbon molecules by about an order of magnitude.[41]

$$[P]_w = [P]_w^0 10^{-0.6n} \quad (9)$$

where n is the number of added carbons, and $[P]_w^0$ is the known water solubility for a derivative with $n = 1$ or 2. We use eq 9 to estimate the water solubility of our probes, taking as the reference value that of 1-ethylpyrene at 23 °C, for which $[P]_w^0 = 1 \times 10^{-7}$ M. In this way, we estimate $[P]_w$ to be 1×10^{-11} M^{-1} for C_8Py, 4×10^{-14} M^{-1} for C_{12}Py, and ca. 10^{-32} M^{-1} for **1**. If we assume the same value of k^+ ($k^+ = 3 \times 10^9$ $M^{-1}s^{-1}$) and n^* ($n^* = 1$) for all of the probes, we obtain an interesting result. By introducing these equilibrium solubilities into eqs 7 and 8, we calculate exit rate constants k^- of 10^{-1} s^{-1} for C_8Py, 4×10^{-4} s^{-1} for C_{12}Py, and 10^{-22} s^{-1} for **1**. For C_8Py and C_{12}Py the predicted values for k^- are of the same order of

magnitude as the experimental values of k_{obs}. Thus there is no need to invoke surfactant assistance for the exchange process of these species of low intrinsic water solubility. In contrast, the exchange rate constant k_{obs} for **1** is more 10^{10} times higher than the predicted k^- value, which confirms that the exchange of this dye must occur by a different mechanism, which we believe is the fission−growth process shown in Chart 1.

Fission−Growth Mechanism. In the top half of Figure 10, we reproduce the slow relaxation data of Lessner et al.[13b] ($1/\tau_{slow}$ vs $[Na^+]$) obtained by pressure-jump experiments as a function of salt and surfactant concentration. The decreasing portion of the data can be described quantitatively by a modification of the AW model to accommodate the counterion contribution to micelle relaxation process for ionic micelles.[13b] They write for this process

$$N_{i-1} + N_1 + (j_i - j_{i-1})N_g = N_i \qquad (10)$$

where N_i denotes the number density of particles of class i (where i represents the number of SDS molecules in those micelles), j_i the number of undissociated monomers per particle, and N_g the number density of counterions. N_1 denotes the number density of free surfactant monomers. The AW mechanism requires a sequence of steps of the type described by eq 10. For this mechanism, the growth reactions at the minimum of the size distribution are rate limiting because of the low concentration of submicellar aggregates in this region.

To explain the crossover to a new process with a rate that increases strongly with increasing $[Na^+]$, these authors propose a new relaxation mechanism. For this new pathway, they invoke a mechanism involving coagulation of submicellar aggregates. This process is written

$$N_k + N_l \underset{b_{kl}}{\overset{a_{kl}}{\rightleftharpoons}} N_i \qquad k + l = i \qquad (11)$$

where k and l denote a class of submicellar aggregates that associate with a rate constant a_{kl}, and i refers to a class of proper micelles. They reasoned that at low ionic strength, this mechanism would be suppressed because of the strong electrostatic repulsion between charged entities. In their model, as the ionic strength of the solution is increased, the potential barrier between aggregates becomes so low that attractive dispersion forces can lead to coagulation. Lessner et al. employed DLVO theory to develop a quantitative description of the influence of the counterion concentration on the association rate constant. This description, which did not take account of the change in aggregation number with increasing salt concentration, successfully predicted a powerlaw increase in $1/\tau_{slow}$ with increasing $[Na^+]$, but predicted an exponent closer to 2 than to 6.

For us, the interesting feature the mechanism of eq 11 is the suggestion that proper micelles undergo spontaneous fragmentation, where b_{kl} describes the rate constant of the reaction $i \rightarrow k + l$.[42] In the notation of Lessner et al., β_i is the sum of dissociation rates of the proper micelles of class i, and β refers to the sum of β_i values, summed over the distribution of proper micelles.[43]

$$\beta_i = \sum_{k,l} b_{kl} \qquad (12a)$$

$$\beta = \frac{\sum_i N_i \beta_i}{\sum_i N_i} \qquad (12b)$$

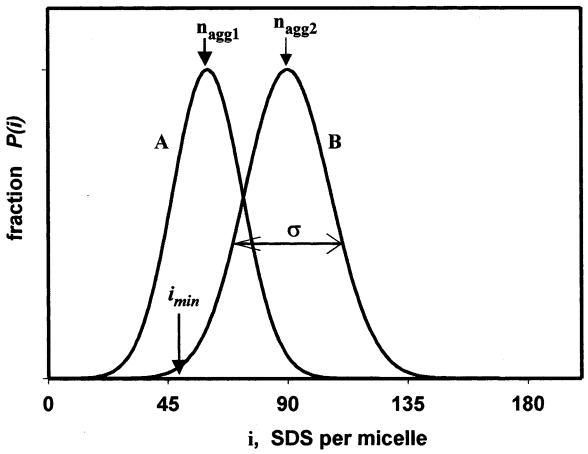

Figure 12. A representation of the size distribution for SDS micelles in the presence of low (A) and higher (B) salt concentrations. Both distributions are assumed to have a Gaussian shape in the vicinity of their maxima. Each distribution is characterized by a mean aggregation number n_{agg} and a distribution width σ. The arrow marked i_{min} represents the smallest micelle that can fragment in such a way that each daughter submicelle can carry a solute such as **1**.

These authors point out that β should be a function of the counterion concentration. They argue that the law of mass action requires the ratio a_{kl}/b_{kl} to be independent of the counterion concentration; thus, b_{kl} should have the same counterion dependence as a_{kl}.

We find (Figure 10, bottom) that k_{obs}, like $1/\tau_{slow}$, increases as a powerlaw with increasing counterion concentration. These data and those in Figure 9 establish that the dominant mechanism of solute exchange for **1** in SDS micelles is fission−growth. The magnitude of the exponent characterizing our data (4) is somewhat smaller than that (6) characterizing the rising portion of the $1/\tau_{slow}$ data. In addition, the k_{obs} values, at comparable $[Na^+]$, are about 100 times smaller than the corresponding values of $1/\tau_{slow}$. There are two reasons why one expects k_{obs} values to be smaller than those of $1/\tau_{slow}$. First, only a fraction of the reactions $i \rightarrow k + l$ will lead to two submicelles large enough that each can carry a molecule of **1**. In contrast, all such reactions will contribute to β. In addition, one can expect the presence of the solute to have a retarding effect on the rate of micelle fission.

The Fission Step. In this section, we examine different models for micelle fission to understand how the rate of this process is enhanced to such an extent by an increase in counterion concentration.

Micelle Polydispersity. The size distribution $P(i)$ of surfactant micelles is characterized by a mean aggregation number n_{agg} and a distribution width σ. $P(i)$ is widely accepted to be Gaussian around the maximum n_{agg}.

$$P(i) = P(n_{agg}) \exp(-(i - n_{agg})^2/2\sigma^2) \qquad (13)$$

From chemical relaxation experiments, Aniansson et al.[11] found $\sigma = 13$ for SDS micelles in the absence of salt.

To explain the exchange of pyrene molecules between dodecylammonium chloride micelles at different salt concentrations, Zana[42] proposed a model based on the influence of salt on the size distribution of micelles present in the solution. The basic idea of this model is that the fission rate will depend on the probability of finding the precursor micelle $P(i)$ and its two daughter submicelles ($P(k)$, $P(l)$) in the solution. In Figure 12, we model the size distribution of SDS micelles under two sets of conditions. These curves were computed with eq 13 for two

different values of n_{agg}, and an identical value of $\sigma = 13$. The distribution with the larger value of n_{agg} refers to a higher salt or salt-plus-surfactant concentration. If the presence of salt increased the micelle polydispersity, the size distribution curve would be broader at higher [Na^+].

According to Zana's model, the broader distribution would favor the formation of submicelles that are described by the low i tail of the distribution. Many authors have argued that polydispersity in the low [salt] regime remains approximately constant.[7,44,45] but increases strongly[7,46]for high [salt], particularly for rodlike micelles regime. Under these circumstances, one cannot explain the increase in fission rate for the low range of [Na^+] in terms of changes in the micelle polydispersity.

Minimum Micelle Size. In Figure 12, we develop a model encompassing the idea that there is a minimum size (i_{min}), which is the smallest submicelle that can transport a molecule of **1** through the aqueous medium. Only micelles with a size higher than ($2i_{min}$) can undergo fission to form two daughter fragments with a size $k,l > i_{min}$. We assume that the size polydispersity of micelles remains constant for the low [Na^+] regime. Addition of salt and SDS shifts the whole size distribution to higher i values without affecting its shape. The two distributions in Figure 12 at different [Na^+] values are characterized by different n_{agg} but the same σ value. In the distribution labeled "B", larger fraction of the micelles can undergo exchange of **1** by the fission−growth mechanism. To test if the "threshold" model can describe the strong dependence of k_{obs} on the [Na^+], we evaluate the predictions of the model using the following assumptions:

(a) Identical fission rates for all events producing $i \geq i_{min}$ and $(i - i_{min}) \geq i_{min}$ and for all salt and SDS concentrations.[47]

(b) Zero exchange rate for events producing micelles with $i < i_{min}$.

(c) Values of n_{agg} calculated with eqs 5 and 6 for [Na^+] between 25 and 140 mM.

(d) Constant micelle polydispersity ($\sigma = 13$)[11] for [Na^+] between 25 and 140 mM and the size distribution calculated with eq 13.

The total fission rate constant is calculated by adding up the fission rates $k_{fr}(i)$ for each of the micelles containing $i > 2i_{min}$ SDS molecules.

$$k_{fr}(i) \propto \sum_{i_{min}}^{i-i_{min}} P(l)P(i-l) \qquad (14)$$

$$k_{fr} \propto \sum_{2i_{min}}^{\infty} P(i)k_{fr}(i) \qquad (15)$$

We selected arbitrary values of i_{min} ranging from 2 to 60. In terms of this simple model, the calculation shows a significant increase in k_{fr} with [Na^+] for low values of [Na^+], particularly for a choice of i_{min} comparable to n_{agg} and a much weaker increase in k_{fr} for high [Na^+]. This is not the case for our experiments, where k_{obs} increases as [Na^+]^4 over the entire range [Na^+] studied here. Under these assumptions, the concept of a "threshold" may contribute to fission, but this model does not describe the strong powerlaw dependence observed for k_{obs} on [Na^+]. The same calculation shows that micelle polydispersity has only a minor effect on k_{fr}.

Shape Fluctuations. In this section we consider the shape and composition of SDS micelles and ask whether fluctuations in that shape could be responsible for the fission process we observe. The most detailed information about the structure of

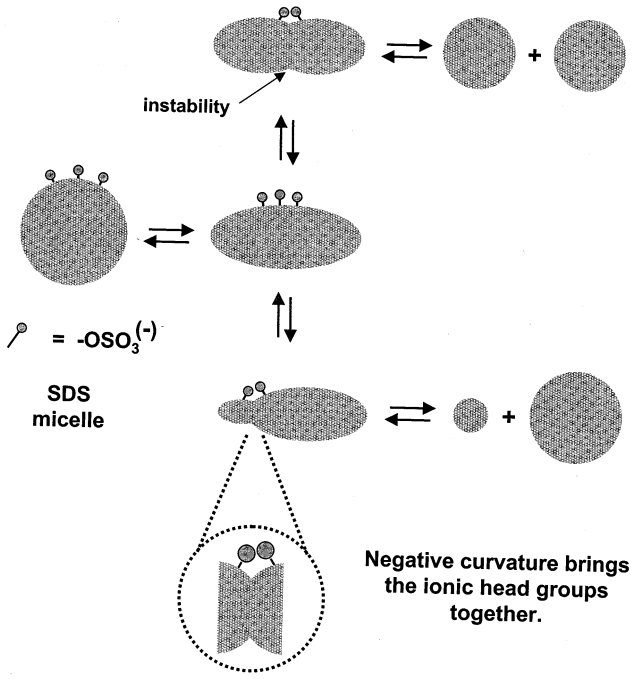

Figure 13. Shape fluctuations in SDS micelles. The surface instabilities that lead to micelle fission force the ionic headgroups into proximity, increasing the Coulombic repulsion between these groups. This interaction is screened at elevated counterion concentration, lowering the free energy barrier to micelle fission.

SDS micelles is provided by the high-resolution neutron scattering experiments reported by Cabane et al.[48] These authors investigated SDS itself and three deuterated samples in water, D_2O, and their mixtures. Their experiments were carried out at an SDS concentration of 2 wt % (70 mM), in the range where we observe significant solute exchange by micelle fission. Under these conditions, the *average* structure of the SDS micelle is that of a dense sphere consisting of 74 SDS molecules with a hydrocarbon core radius $\langle R \rangle = 1.84$ nm. At high resolution, fluctuations away from the average structure were observed. When the internal structure of the core was not resolved, their experiments measured the dispersion in the aggregation number ($\sigma_n/n_{agg} = 0.33$) and the radius ($(\sigma_R/\langle R \rangle = 0.1$). Information about the internal structure of the micelles was provided by experiments with SDS deuterium-labeled at specific sites. Measurements with SDS-12d_3 show that the methyl groups are not concentrated in the center of a sphere. Corresponding experiments with SDS-3d_2 indicate that the γ-CH_2 groups are not confined to a spherical shell. To account for these observations, the authors conclude that fluctuations in micelle shape contribute to the signals they measure. They infer that the most important of these are probably the lowest order spherical harmonics (i.e., $l = 2$), leading to disklike shapes in which the terminal methyl group and the γ-CH_2 groups have similar spatial distributions.

In Figure 13 we suggest that large amplitude fluctuations promote fission through a "pinching off" process that create two smaller micelles. Surface instabilities are transient states of higher energy. In SDS, the creation of a surface instability requires close approach of the negatively charged headgroups at the locus of the instability. Headgroup repulsion plays an important role in determining micelle size.[36] As the counterion concentration is increased, there is an increase in the extent of ion pairing and screening of Coulombic interactions between headgroups. Both factors reduce the net effective headgroup size. From this perspective, a micelle surface fluctuation that

created an instability of the sort shown in Figure 13 would result in strong electrostatic repulsion in this zone, which in turn would act as a barrier to creation of these instabilities, and consequently, as a barrier to fission.

This model provides a qualitative explanation for the dependence of k_{obs} on [Na^+]. In the absence of salt, surface instabilities are difficult to form, because the close approach of the negative charges at the site of the instability requires high energy to overcome the electrostatic forces. This high barrier explains the extremely low fission rates observed in the absence of salt. The addition of [Na^+] screens the electrostatic forces, which lowers the energy for the creation of these instabilities, and promotes an enhancement of the fission rate. These instabilities become important for high counterion concentrations. They may be related to the fluctuations that occur prior to the transition from spherical to wormlike micelles, which takes place at [Na^+] $\geq$ 0.5 M.

Summary

Time scan fluorescence experiments with a water-insoluble pyrene-containing probe **1** allow us to follow the rate of solute exchange in SDS micelles as a function of surfactant and salt concentration. This rate is remarkably sensitive to the Na^+ concentration, increasing as [Na^+]^4. The mechanism of solute exchange for **1** involves spontaneous micelle fission, followed by growth of the daughter micelles back to normal micelles. We imagine that only a fraction of fission events of micelles containing two molecules of **1** form two daughter submicelles large enough that each can carry one of the molecules of **1**. Thus the exchange rates we measure are substantially slower than the slow relaxation rates of SDS micelles reported by the Kahlweit group[13] at corresponding sodium ion concentration.

We propose a mechanism for the fission process, caused by surface fluctuations of the micelle core. When the amplitude of these fluctuations are large enough, the probability of "pinching off" a subunit becomes significant. Surface fluctuations that lead to fission bring headgroups into close contact. These deep fluctuations are opposed by electrostatic repulsions between adjacent headgroups. Increased counterion concentration helps screen these interactions and thus amplify the fission rate.

Acknowledgment. The authors thank ICI, ICI Canada, and NSERC Canada for their support of this research.

References and Notes

(1) Quina, F. H.; Nassar, P. M.; Bonilha, J. B. S.; Bales, B. L. *J. Phys. Chem.* **1995**, *99*, 17028.

(2) Bezzobotnov, V. Y.; Borbely, S.; Cser, L.; Farago, B.; Gladkih, I. A.; Ostanevich, Y. M. *J. Phys. Chem.* **1988**, *92*, 5738.

(3) Bales, B. L.; Almgren, M. *J. Phys. Chem.* **1995**, *99*, 15153.

(4) Hayashi, S.; Ikeda, S. *J. Phys. Chem.* **1980**, *84*, 744.

(5) Missel, P. J.; Mazer, A. N.; Carey, M. C.; Benedek, G. B. *J. Phys. Chem.* **1989**, *93*, 8354.

(6) Bales, B. L.; Messina, L.; Vidal, A.; Peric, M.; Nascimento, O. R. *J. Phys. Chem. B* **1998**, *102*, 10347.

(7) Siemiarczuk, A.; Ware, W. R.; Liu, Y. S. *J. Phys. Chem.* **1993**, *97*, 8082.

(8) Zana, R. In *Surfactant Solutions: New Method of Investigation*; Zana, R., Ed., Marcel Dekker: New York, 1987.

(9) For reviews of dynamic processes in micelles, see: (a) Muller, N. In *Solution Chemistry of Surfactants*; Mittal, K. L., Ed.; Plenum: New York, 1979; Vol. I, pp 267−295. (b) Gormally, J.; Gettins, W. J.; Wyn-Jones, E. In *Molecular Interactions*; Wiley: New York, 1980; Vol. 2, pp 143−177. (c) Lang, J.; Zana, R. In *Surfactant Solutions: New Methods of Investigation*; Zana, R., Ed.; Marcel Dekker: New York, 1987; pp 405−452. (d) Huibers, P. D. T.; Oh, S. G.; Shah, D. O. In *Surfactants in Solution*; Chattopadhay, A. K.; Mittal, K. L., Eds., Marcel Dekker: New York, 1995; Vol. 64, pp 105−121.

(10) Lang, J.; Tondre, C.; Zana, R.; Bauer, H.; Hoffmann, H.; Ulbricht, W. *J. Phys. Chem.* **1975**, *79*, 275.

(11) Aniansson, E. A. G.; Wall, S. N. *J. Phys. Chem.* **1974**, *78*, 1024−1030; *J. Phys. Chem.* **1975**, *75*, 857−858.

(12) Aniansson, E. A. G.; Wall, S. N.; Almgren, M.; Hoffmann, H.; Kielmann, H.; Ulbricht, W.; Zana, R.; Lang, J.; Tondre, C. *J. Phys. Chem.* **1976**, *80*, 905.

(13) a) Lessner, E.; Teubner, M.; Kahlweit, M. *J. Phys. Chem.* **1981**, *85*, 1529; b) **1981**, *85*, 3167.

(14) Rharbi, Y.; Winnik, M. A. *J. Am. Chem. Soc.* **2002**, *124*, 2082.

(15) Barzykin, A. V.; Seki, K.; Tachiya, M. *Adv. Colloid Interface Sci.* **2001**, *89*, 47.

(16) Gehlen, M. H.; De Schryver, F. C. *Chem. Rev.* **1993**, *93*, 199.

(17) Infelta, P. P.; Grätzel, M.; Thomas, J. K. *J. Phys. Chem.* **1974**, *78*, 190.

(18) Bolt, J. D.; Turro, N. J. *J. Phys. Chem.* **1981**, *85*, 4029.

(19) Almgren, M.; Grieser, F.; Thomas, J. K. *J. Am. Chem. Soc.* **1979**, *101*, 2021.

(20) Scaiano, J. C.; Selwyn, J. C. *Can. J. Chem.* **1981**, *59*, 2368.

(21) Selwyn, J. C.; Scaiano, J. C. *Can. J. Chem.* **1981**, *59*, 663.

(22) Pileni, M. P.; Grätzel, M. *J. Phys. Chem.* **1980**, *84*, 1822.

(23) Hruska, Z.; Piton, Mark, Yekta, A.; Duhamel, J.; Winnik, M. A.; Riess, G.; Croucher, M. D. *Macromolecules* **1993**, *26*, 1825.

(24) Rharbi, Y.; Winnik, M. A. *Adv. Colloid Interface Sci.* **2001**, *89*, 25.

(25) Rharbi, Y.; Winnik, M. A.; Hahn, K. G. *Langmuir* **1999**, *15*, 4697.

(26) Rharbi, Y.; Bechthold, N.; Landfester, K.; Salzman, A.; Winnik, M. A. *Langmuir* **2003** *19*, 10.

(27) Hilczer, M.; Barzykin, A. V.; Tachiya M. *Langmuir* **2001**, *14*, 4196−4201.

(28) Rharbi, Y.; Li, M.; Winnik, M. A.; Hahn, K. G. *J. Am. Chem. Soc.* **2000**, *122*, 6242.

(29) Bohne, C.; Konuk, R.; Scaiano, J. C. *Chem. Phys. Lett.* **1988**, *152*, 156.

(30) Infelta, P. P.; Gräzel, M.; Thomas, J. K. *J. Phys. Chem.* **1974**, *78*, 190;. Tachiya, M. *Chem. Phys. Lett.* **1975**, *33*, 289. Atik, S. S.; Mikki, N.; Singer, L. A. *Chem. Phys. Lett.* **1979**, *67*, 75.

(31) Dubin, P. L.; Principi, B. A.; Smith, M. A.; Fallon, *J. Colloid Interface Sci.* **1989**, *127*, 558.

(32) Rharbi, Y.; Kitaev, V.; Winnik, M. A.; Hahn, K. G. *Langmuir* **1999**, *15*, 2259.

(33) Zachariasse, K. A. In *Surfactant in Solution*; Mittal, K. L, Ed.; Plenum Press: New York, 1989; Vol 7, p 79.

(34) Hoffmann, H.; Kielmann, H.; Pavlovic, D.; Platz, G.; Ulbricht, W. *J. Colloid Interface Sci.* **1981**, *80*, 237.

(35) The 3-fold slower entry rate for SDS reflects the Coulombic effect on the entry process for ionic surfactants.

(36) Israelachvili, J. N. *Intermolecular & Surface Forces*, 2nd ed.; Academic Press: London, 1992.

(37) Lianos, P.; Zana, R. *J. Phys. Chem.* **1980**, *84*, 3339.

(38) Sasaki, T.; Hattori, M.; Sasaki, J.; Nukina, K. *Bull. Chem. Soc. Jpn.* **1975**, *48*, 1397.

(39) Hall, D. G. *J. Chem. Soc., Faraday Trans.* **1981**, *77*, 1121.

(40) Rharbi, Y.; Chen, L.; Winnik, M. A. Manuscript in preparation.

(41) Taisne, L.; Walstra, P.; Cabane, B. *J. Colloid Interface Sci.* **1996**, *184*, 378.

(42) Malliaris et al. also postulated a similar mechanism when studying exchange of pyrene (on a much faster time scale) between dodecylammonium chloride micelles. Malliaris, A.; Lang, J.; Zana, R. *J. Phys. Chem.* **1986**, *90*, 655.

(43) In the notation of Lessner et al. (ref 42), $\beta_i = \sum_{k,l} b_{kl}$ (with $i - k - l = 0$), and $\beta = \sum \beta_i \bar{N}_i / \bar{Z}$, where N_i is the number density of surfactant monomers and Z is $\beta = \beta_o / f$; see p 3171.

(44) Dutt, G. B.; van Stam, J.; DeSchryver, F. C. *Langmuir* **1997**, *101*, 11957.

(45) Hall, D. G. *Langmuir* **1999**, *15*, 3483.

(46) Almgren, M.; Gimel, J. C.; Wang, K.; Karlsson, G.; Edwards, K.; Brown, W.; Mortensen, K. *J. Colloid Interface Sci.* **1998**, *202*, 222.

(47) In the Halperin and Alexander model of block copolymer micelles, the barrier to fission is modeled in term of the increase in surface area created as a result of creating two smaller spheres. From this perspective, for a micelle made up of f block copolymers, they predict the largest activation energy for the symmetric fission into two submicelles containing $f/2$ block copolymers. Halperin, A.; Alexander, S. *Macromolecules* **1989**, *22*, 2403.

(48) Cabane, B.; Duplessix, R.; Zemb, T. *J. Phys.* **1985**, *46*, 2161−2178.